

## RESPONSE TO REVIEWERS' COMMENTS

**Journal:** Sensors & Actuators: B. Chemical

**Ms. Ref. No.:** SNB-D-18-06556

**Title:** Paper-based electrochemical transducer modified with nanomaterials for mercury determination in environmental waters

**Authors:** A. Sánchez-Calvo, M.T. Fernández-Abedul, M.C. Blanco-López\*, A. Costa-García\*

We would like to thank the editor and reviewers for their constructive comments on our manuscript. The following changes have been made.

### REVIEWER #1:

*1. When referring to metals (including Hg (II)) please use the cationic form (i.e Cd(II), Pb(II), Cu(II), Zn(II) instead of cadmium, lead, copper and zinc) throughout the text*

The manuscript was modified to referring all the metals mentioned as the cationic form.

*2. The proposed transducers are obviously for single use. The life-time of the underlying ceramic SPE (in terms of number of analyses it can sustain) should be also reported*

We have included the average use of the underlying ceramic SPE in the paragraph 2.2 of page lines 122-124. It can be higher for skilled operators:

“The SPE can be reused for an average of 7-8 measurements with no effect on the structure of the platform”

*3. The procedure for placing the sample on the WE is not specified. If a sample drop is applied on the electrode surface, its volume should be reported.*

The following sentence has been added (line 167): 40 mL of sample solution were deposited on the electrochemical cell. Figure 1 was also modified to include the volumes of sample aliquots and nanomaterial suspension added on the electrode surface

*4. Page 10, 2nd paragraph: "Increasing concentrations of KCl resulted on voltammograms with lower capacitance and better defined and more intense peaks (Figure 3)". However, Figure 3 compares the CVs with different modifiers and not the KCl concentration. Please correct. Also, no discussion on the findings of Fig. 3 can be found.*

We have corrected the mistake by referring the Figure 2 instead of Figure 3 (line 206, page 7) to explain the influence of the KCl concentration. Figure 3 was used as reference at the discussion of the assignation of electrochemical peaks at page 7, lines 189-198. Discussion has been completed at lines 211-215.

*5. Figure 4: the concentration ranges in the 2 types of electrodes are different. Is there a reason for this?*

Firstly, both types of electrodes were used to study the same concentration range. However, the sensitivity of rGO/AuNPs paper-based electrode is lower, so the lowest concentration could not be determined. The different linear concentration ranges, according- the sensibility of each modified electrode are shown at Figure 4.

*6. Figure 12: a caption for Fig. 6 appears. However, no Figure 6 exists.*

The caption referred to Figure 5. We have corrected the mistake.

*7. Figure 12: it is stated that "Figure 5 shows the results of this interference study" but these are shown in Table 1.*

We have corrected the mistake. Figure 5 showed matrix effect.

*8. Figure 5: the standard addition straight line should be extrapolated to the point where it intersects with the x axis to show the concentration determined by the analysis. How was the recovery value derived?*

Figure 5 was modified to include the extrapolations, showing how the concentration of the sample was calculated. Recovery values were the percentage of concentration found (with the calibration line) related to the known spiked concentration on river water.

*9. Table 1 is not necessary and can be deleted*

Table 1 has been deleted. The absence of interference from Pb (II), Cd (II), Zn (II) and Cu (II) was reported (lines 296-302).

1

2

3

4 **Paper-based electrochemical transducer modified with nanomaterials**  
5 **for mercury determination in environmental waters**

6 A. Sánchez-Calvo, M.T. Fernández-Abedul, M.C. Blanco-López\*, A. Costa-García\*

7 *Departamento de Química Física y Analítica, Facultad de Química, Universidad de*  
8 *Oviedo, 33006 Oviedo, Spain*

9

10

11 \*Corresponding authors: [cblanco@uniovi.es](mailto:cblanco@uniovi.es)

12 [costa@uniovi.es](mailto:costa@uniovi.es)

13

14 **Abstract**

15 A sensor for Hg (II) determination in water was developed by using paper working  
16 electrodes modified with nanomaterials. The cellulose matrix was modified with  
17 hybrids of carbon nanofibers (CNFs) or reduced graphene oxide (rGO) and gold  
18 nanoparticles (AuNPs), in order to increase the selectivity and sensitivity. The AuNPs  
19 helped the electrodeposition of Hg (II) at more positive potentials, due to their affinity  
20 for mercury. The determination was possible up to 1.2  $\mu\text{M}$  with no interference of other  
21 heavy metals such as Cd (II), Pb (II), Cu (II) and Zn (II). The CNFs/AuNPs modified  
22 paper-based electrode was the most sensitive option with a detection limit of 30 nM.  
23 River water samples were evaluated by the standard addition method.

24

25 **Keywords**

26 Paper electrodes, carbon nanomaterials, gold nanoparticles, mercury, low-cost analysis,  
27 decentralized analysis

28

## 29 1. Introduction

30 Heavy metals are becoming a high concern in terms of human health and  
31 environment. Excessive concentration in drinking water may result in chronic diseases  
32 or even mortality [1–3]. One of the most hazardous is Hg (II). This element can be  
33 present in organic and inorganic forms, being both dangerous because of their toxicity  
34 and bio-accumulation in many species [4–6].

35 Organizations like World Health Organization (WHO) have established 30 nM  
36 as the top limit value for drinking water [7]. This has carried along the need for  
37 determination methods with high sensitivity. Some of the available methods include  
38 spectroscopic techniques such as Cold Vapour Atomic Absorption Spectroscopy  
39 (CVAAS) [8] or Inductively Coupled Plasma Mass Spectrometry (ICP-MS) [9], but  
40 these procedures are not suitable for *in situ* analysis because they require expensive  
41 instruments and qualified people. Electroanalytical methods, in contrast, allow  
42 simultaneous determination of several heavy metals at low cost, with minimum volume  
43 of sample and easy-to-use instruments [10]. Most of the heavy metals, like Hg (II) or  
44 Pb (II) can be determined by Anodic Stripping Voltammetry (ASV) [11,12]. Electrodes  
45 can be modified with conductive materials like polymers or with biological compounds  
46 to increase their conductivity and improve the sensitivity and selectivity of the sensors  
47 [13–16].

48 For the purpose of Hg (II) determination, gold is often the preferred electrodic  
49 material, because of its strong affinity for Hg. This can be used to enhance the  
50 preconcentration effect during the accumulation step [17,18]. It has been used as a bulk  
51 electrode or in the form of microdisks, but as gold nanoparticles (AuNPs), their high  
52 surface area-to-volume ratio results in both sensitivity and selectivity improvements  
53 [19–22]. AuNPs can be synthesized *in situ* by electrodeposition [23–25].

54 Sensitive Hg (II) determinations in water were achieved with glassy carbon  
55 [26,27], or screen-printed carbon electrodes (SPCEs) [28] modified with AuNPs and/or  
56 nanohybrids. SPCEs have advantages such as low cost and little amount of sample and  
57 reagents required. However, most of the ceramic SPCEs designed are usually discarded  
58 after one measurement because of the fouling of the surface. In recent years, efforts  
59 have been made to develop low-cost alternatives more feasible for developing countries  
60 such as transparency films [29] or paper [30–33].

61 Paper is mainly composed of cellulose fibres which can be modified by the  
62 addition of hydrophobic materials such as wax, with the aim to form barriers that define  
63 the electrochemical cell. Cellulose can be modified with conductive ink to allow the  
64 study of electrochemical probes [34,35]. It can also be modified with nanoparticles  
65 increasing the conductivity and selectivity of the method [36], it is inexpensive and easy  
66 to destroy after use.

67 Here, we have studied the utility of a nanostructured paper-based electrode as  
68 the working electrode of a simple and low-cost platform for Hg (II) in water. The paper  
69 substrate was modified with carbon materials such as graphene-oxide (GO) or carbon

70 nanofibers (CNF) and with gold nanoparticles (AuNPs) to obtain a new and “*easy-to-*  
71 *make*” working electrode. It was connected to the auxiliary and reference electrodes of a  
72 screen-printed card having its own working electrode isolated from the sample. This  
73 ensures its use without any interference, and the stability required in order to apply  
74 electrochemical treatments.

## 75 **2. Experimental**

### 76 **2.1. Materials and Methods**

77 Potassium chloride, Cd (II) standard, Zn (II) standard and HCl were purchased  
78 from Merck KGaA (Germany). Potassium hexacyanoferrate (II), trihydrate potassium  
79 hexacyanoferrate (III), tris (hydroxymethyl)aminomethane, Pb (II) standard, Cu (II)  
80 nitrate trihydrate and Hg (II) acetate were purchased from Sigma-Aldrich (USA). Water  
81 used was obtained from a Millipore Milli-Q purification system (Millipore Direct-Q® 3  
82 U) from Millipore Ibérica S.A (Madrid, Spain).

83 Graphene oxides (GOs) were obtained from Instituto Nacional del Carbón  
84 (INCAR, CSIC, Spain). Graphite was obtained following a heat treatment at 2800°C.  
85 Then, a modified Hummers method was used to transform it into GO [37]. A 1 mg/L  
86 solution on ultrapure water is the final product. Nanofibers were obtained from Grupo  
87 Antolin (Spain). Carbon paste (ref. C10903P14) was acquired from Gwent group  
88 (United Kingdom).

89 Screen-printed electrode cards were obtained from Dropsens S.L. (SPCEs, ref.  
90 DRP-110, Spain). Working and auxiliary electrodes are made of carbon ink, with a  
91 pseudoreference electrode made of silver. A DSC connector (ref DRP-DSC) from the  
92 same company was used to connect them with the potentiostat.

93 A wax printer (Xerox Colorcube 8570) was used to print the paper. Wax was  
94 melted using a thermostat model (Nabertherm d-2804). The spray adhesive 3M Spray  
95 Mount™ was acquired from local stores.

96 Electrochemical measurements were carried out with a potentiostat (Autolab,  
97 PGSTAT 10) controlled by the Autolab GPES software. Cyclic voltammetry was used  
98 to study the influence of gold nanoparticles (AuNPs) and chloride ions on the  
99 electrochemical process of mercury ( $E_i = -0.35$  V,  $E_f = +0.60$  V,  $E_s = 2$  mV and  $v = 50$   
100 mV/s).

### 101 **2.2. Design of paper-based electrodes**

102 Whatman Grade 1 chromatographic paper was chosen as a cellulose substrate. A  
103 wax printer was used to print hydrophobic wax patterns on the paper. Paper patterns  
104 designs were made using Inkscape software. After melting the wax at 80°C and cooling  
105 at room temperature, the paper was modified by addition of 2 µL of carbon ink solution  
106 by drop casting on one of the sides. In this way, a side was covered by ink (bottom side)  
107 and the other side was used to add nanomaterial and sample solutions (upper side). The  
108 carbon ink used to modify the cellulose paper was made by dispersion of the

109 commercial carbon paste in anhydrous N,N-dimethylformamide (DMF) (concentration  
110 of 30 % (w/w)) in an ultrasound bath for one hour.

111 Following a procedure previously developed in our group [34,38], the working  
112 electrode (WE) of the screen-printed platform as well as the ceramic surface that is  
113 located between the WE and auxiliary (AE) and reference (RE) electrodes, were  
114 covered by the cellulosic electrode. Every paper electrode was cut to obtain a circle with  
115 an area of 4 mm<sup>2</sup> as shown in Figure 1. The carbon ink of the paper working electrode  
116 was covered by a protector. Then, an adhesive was sprayed and after removing the  
117 cover, the cellulosic electrode was placed over the WE of a screen-printed electrode  
118 card (SPE), in such a way that the carbon ink of the paper electrode contacted the WE of  
119 the SPE, as shown in Figure 1 B. With this methodology, there was no any interference  
120 from the adhesive spray. Before measurements were made, full overlap was verified.  
121 The solution was added on the upper side of the paper electrode that was not contacting  
122 the WE of the SPE, making sure there were no interferences from previous  
123 measurements. Then, the WE of the SPE remained unmodified, acting only as  
124 connection [34–36, 38]. The SPE can be reused for an average of 7-8 measurements  
125 with no effect on the structure of the platform.

### 126 **2.3. Modification with carbon nanomaterials and gold nanoparticles**

127 Paper electrodes with carbon ink were modified with a combination of carbon  
128 nanomaterials followed by a generation of gold nanoparticles (AuNPs). Both procedures  
129 are shown in Figure 1 (C1 and C2). Carbon nanomaterials were added before placing  
130 the paper electrode over the screen-printed card, whereas gold nanoparticles were  
131 generated afterwards. Graphene oxide added was also electrochemically reduced before  
132 the generation of gold nanoparticles. Hybrids of carbon nanomaterials with AuNPs were  
133 investigated to optimize the detection.

#### 134 2.3.1. Modification with carbon nanofibers (CNFs)

135 Suspensions of CNFs were prepared in ultrapure water by solving an amount of  
136 CNFs in an ultrasonic bath for 1 hour. An aliquot of 2 µL of a 1 mg/mL nanofiber  
137 suspension was deposited onto the upper part of the paper and left to dry at room  
138 temperature before placing it on the screen-printed electrode card.

#### 139 2.3.2. Modification with graphene oxide (GO)

140 Aliquots of 6 µL of GO (100 mg/L) were added to the upper part of the paper  
141 and left to dry at room temperature. Graphene oxide needs to be reduced in order to  
142 remove oxide and hydroxide groups. Therefore, after placing it over the screen-printed  
143 electrode card, a constant cathodic current of -100 µA was applied and the reduction  
144 process was followed chronopotentiometrically in 0.1 M NaOH, according to a  
145 procedure developed in our research group to generate reduced graphene oxide (rGO)  
146 [37].

#### 147 2.3.3. Modification with gold nanoparticles (AuNPs)

148 AuNPs were synthesized in situ by a method previously developed in our  
149 research group for screen-printed carbon electrodes [36] and successfully tested in  
150 paper-based electrodes [34,36]. AuNPs were electrogenerated after deposition of 40  $\mu\text{L}$   
151 of 1 mM  $\text{AuCl}_4^-$  on a cellulose disk overlaying the surface of the working electrode, at  
152 the screen-printed card. A current of  $-100 \mu\text{A}$  was applied and the corresponding  
153 chronopotentiogram was recorded.

154

### INSERT FIGURE 1

155 **Fig. 1** Schematic diagram showing the preparation of the paper electrodes used. (A) Modification of  
156 cellulose substrate by addition of carbon ink on one side. As result, the platform has two visually different  
157 sides. Solution is added with a micropipette through the upper side. (B) Overlapping process of the  
158 bottom (ink) side of the paper electrode, on the screen-printed card. (C) Modification of the paper  
159 electrode with 1) CNFs and AuNPs, and 2) rGO and AuNPs.

160

## 2.4. River water analysis

161 Water from river Nora (Asturias, Spain) was collected for mercury  
162 determination. The sample was spiked with 1  $\mu\text{M}$  of mercury (II) acetate. For the  
163 determination, standard additions were made by adding 100, 200 and 400  $\mu\text{L}$  of 20  $\mu\text{M}$   
164 Hg (II) standard (in 0.1 M HCl + 0.9 M KCl, i.e. 1 M  $\text{Cl}^-$  background electrolyte) to 300  
165  $\mu\text{L}$  of the spiked sample and making up to 1 mL with 1 M  $\text{Cl}^-$  background electrolyte.

166 Real sample measurements and calibration plots were made by linear sweep  
167 voltammetry. 40  $\mu\text{L}$  of sample solution were deposited on the electrochemical cell. Hg  
168 (II) in the samples was preconcentrated by applying a potential of +0.2 V for 600 s.  
169 Then, the reduced mercury was stripped from the electrode surface by scanning the  
170 potential in the anodic direction ( $E_i = +0.2 \text{ V}$ ,  $E_f = +0.6 \text{ V}$ ,  $E_s = 2 \text{ mV}$  and  $v = 50 \text{ mV/s}$ ).

171

## 3. Results and discussions

172

### 3.1. Electrochemical behaviour of Hg (II) at carbon nanomaterials-AuNPs modified paper-based electrodes

173

174

175

176

177

178

179

180

181

182

183

184

185

186

187

188

The electrochemical processes of mercury on paper-based electrodes modified with both carbon nanomaterials and gold nanoparticles were studied by cyclic voltammetry using a  $10^{-4} \text{ M}$  Hg (II) acetate solution in 0.1 M HCl. This analyte was preconcentrated by applying a reduction potential of  $-0.35 \text{ V}$  for 480 s, and then the potential was scanned in the positive sense. Figure 2 shows the voltammograms obtained in CNFs/AuNPs paper-based electrodes. Different amounts of KCl were added to improve the conductivity without increasing the acidity of the solution. This could remove the adhesive and release the paper substrate from the screen-printed card. The three anodic peaks observed (in 0.1 M HCl + 0.9 M KCl) at +41 (A3), +235 (A2) and +426 (A1) mV seem to form a redox pair with the three corresponding cathodic peaks at  $-14.8$  (C3), +230 (C2) and +400 (C1) mV. The voltammogram is similar to that obtained by using AuNPs-SPCEs [37]. As it was described there, the redox pairs A1/C1 and A2/C2 correspond to the adsorption of Hg (II) ions on the surface of AuNPs, making an amalgam in a process called underpotential deposition (UPD), only observed



189 at electrodes modified with AuNPs, as shown in Figure 3 for these paper electrodes.  
190 The UPD corresponds to an electrochemical process that takes place at a more positive  
191 potential than the reversible Nernst potential for the formation of bulk metal. The first  
192 UPD process (A1/C1) occurs at +413 mV ( $E_{pa} + E_{pc}/2$ ), and a second UPD (A2/C2) at  
193 +230 mV is normally observed when all AuNPs are saturated of mercury atoms, having  
194 hence a weaker influence. The anodic peak A3 at +41 mV was also observed at  
195 unmodified paper electrodes, and therefore it was assigned to the bulk deposition of Hg  
196 at the carbon ink [39]. It was also present in paper modified with CNF and rGO (Figure  
197 3). The other anodic peak, that appears at a lower potential, could be related to the  
198 presence of chloride ions in the medium [40].

199

200

## INSERT FIGURE 2

201 **Fig. 2** Cyclic voltammograms obtained at CNFs/AuNPs electrodes in a  $10^{-4}$  M Hg (II) acetate solution in  
202 (A) 0.1 M HCl, (B) 0.1 M HCl + 0.9 M KCl and (C) 0.1 M HCl + 1.9 M KCl solutions. (D) Background  
203 voltammogram recorded in a 0.1 M HCl + 0.9 M KCl solution.

204

205 Increasing concentrations of KCl resulted on voltammograms with lower  
206 capacitance and better defined and more intense peaks (Figure 2). The potential of the  
207 processes decreases slightly using more concentrated electrolyte, indicating that the  
208 oxidation processes result favoured. The best results were obtained with a 1 M  
209 concentration of chloride ion. Higher concentrations did not make any improvement.  
210 Then, a 1 M of chloride ion (i.e., 0.1 M HCl + 0.9 M KCl) solution was employed as  
211 background electrolyte for the remainder of the work. UPDs peaks were better defined  
212 for CNFs/AuNPs paper-based electrodes in comparison with those modified with  
213 rGO/AuNPs. This could be due to the higher capacitance of the cellulose matrix  
214 modified with reduced graphene oxide. The effect of the carbon nanomaterials on the  
215 capacitive currents in absence of AuNPs can also be observed in Figure 3.

216

217 The UPDs at AuNPs nanostructured electrodes are advantageous for sensitive  
218 and selective determination of low concentrations of Hg. Bulk deposition was only  
219 observed at higher concentrations. Bulk deposition at CNFs and rGO paper electrodes  
220 has low reproducibility and less selectivity in comparison with paper electrodes  
221 modified also with AuNPs, so they were not considered. On the other hand, the  
222 modification with carbon nanomaterials increases the reproducibility of the  
223 electrodeposition of gold nanoparticles. For this reason, the use of AuNPs paper  
224 electrodes with no carbon nanomaterials was discarded. In conclusion, a hybrid  
225 nanostructuring resulted then more convenient. The first UPD (A1/C1) was chosen for  
226 the development of the sensor for the determination of mercury (II) ions by anodic  
227 stripping voltammetry. Then, mercury was preconcentrated (reduction of Hg (II) to Hg  
228 (0)) at a potential more negative than C1. Then, an anodic potential sweep was applied  
229 for Hg redissolution (from Hg (0) to Hg (II)). The analytical signal measured was the  
intensity of the A1 peak current.

230

231

### INSERT FIGURE 3

232 **Fig.3** Cyclic voltammograms for a  $10^{-4}$  M Hg (II) acetate solution at A) CNFs/AuNPs, (B) CNFs, (C)  
233 rGO/AuNPs and (D) rGO modified electrodes. Background electrolyte: 0.1 M HCl + 0.9 M KCl solution.

234

### 235 3.2. Study of the determination of Hg (II) at carbon nanomaterials / AuNPs 236 paper-based electrodes

237 We have optimized the electrogeneration of AuNPs in paper electrodes modified  
238 with carbon nanofibers (CNFs) or reduced graphene oxide (rGO) by  
239 chronopotentiometry. Current intensity of  $-100 \mu\text{A}$  was applied at different time  
240 intervals. A value of 360 s resulted on the highest oxidation peak for mercury, around  
241  $+380 \text{ mV}$ . ( $E_{\text{pa}}$  for the A1 process). The difference on the potential value with respect to  
242 the anodic peak A1 could be due to the influence of the ion chloride  $\text{Cl}^-$  on the  
243 pseudoreference electrode of Ag at the screen-printed card. It could partially form AgCl,  
244 changing the redox potential of mercury ions, therefore. Hg (II) was then determined by  
245 anodic stripping voltammetry, measuring the current intensity of the anodic peak around  
246  $+380 \text{ mV}$ . A potential of  $+200 \text{ mV}$  was chosen for studying the influence of different  
247 electrodeposition times for both procedures (CNFs/AuNPs and rGO/AuNPs). Square  
248 wave voltammetry (SWV), differential pulse voltammetry (DPV) and linear sweep  
249 voltammetry (LSV) were evaluated. The most reproducible results were obtained with  
250 linear sweep voltammetry, by applying a potential of  $+200 \text{ mV}$  for 600 s (480 s for  
251 graphene oxide) as a preconcentrating step, followed by an anodic potential scan from  
252  $+0.2$  to  $+0.6 \text{ V}$ .

253 To compare carbon nanomaterials and study the sensitivity of the analytical  
254 methodologies, both types of modified paper electrodes (CNFs/AuNPs and  
255 rGO/AuNPs) were tested for different concentrations of mercury (II) acetate. Figure 4  
256 shows two calibration plots for the hybrid structures CNFs/AuNPs and rGO/AuNPs.  
257 The best fit corresponded to the former, with CNFs/AuNPs (calibration line:  $I_{\text{pa}} (\mu\text{A}) =$   
258  $0.4461 [\text{Hg}(\text{II})] - 0.0305$ ,  $R^2 = 0.9969$ ). The linear range was comprised between 0.1  
259 and  $1.2 \mu\text{M}$ . The limit of detection (LOD) for the hybrid nanostructuration with  
260 CNFs/AuNPs was calculated as  $30 \text{ nM}$  by the formula  $3S_a/m$ , where  $S_a$  is the standard  
261 deviation of the blank and  $m$  is the slope of the calibration line, using the lower range  
262 concentration values. The capacitive current was lower for CNFs/AuNPs paper-based  
263 electrodes. In conclusion, this was the system chosen to analyse the river water samples.

264

265

### INSERT FIGURE 4

266 **Fig. 4** (A) Calibration plots for mercury (II) acetate in CNF/AuNPs and rGO/AuNPs paper-based  
267 electrodes. (B) Linear sweep voltammograms in CNF/AuNPs paper-based electrodes at increasing  
268 concentrations of mercury (II) acetate in a 0.1 M HCl + 0.9 M KCl solution.

269

270 Water samples were taken from river Nora (Asturias, Spain). Mercury was not  
271 detected. Then, aliquots for mercury determination at the CNFs/AuNPs and  
272 rGO/AuNPs paper-based electrodes were prepared by spiking 1  $\mu\text{M}$  of mercury (II)  
273 acetate. Solutions were analysed by the anodic stripping voltammetry method  
274 developed (Section 2.4). For the determination, standard additions were made to  
275 aliquots of 300  $\mu\text{L}$  of the spiked sample. Then, different volumes of Hg (II) standard in  
276 1M  $\text{Cl}^-$  background electrolyte were added. The comparison of the standard addition  
277 line of the spiked samples with the calibration plot line indicated matrix effects (Figure  
278 5). This can be explained because of the different compounds from the matrix river  
279 which can alter the background of the solution and its conductivity. However, the  
280 method is based on the UPD electrodeposition of mercury (II) ions at the AuNPs  
281 surface, and subsequent anodic redissolution. The interference study at next section  
282 shows that the determination is quite selective nevertheless. Moreover, matrix effects  
283 could be corrected by using the standard addition method. Results indicated that 91% of  
284 the spiked concentration was recovered, being still a suitable alternative to study real  
285 samples. Samples were also analysed by the method previously developed at AuNPs  
286 and SPCEs [39]. The results obtained at the SPCEs (97%) were consistent with those  
287 obtained at paper-based electrodes developed in this study.

288

289

## INSERT FIGURE 5

290

291 **Fig.5** (A) Calibration plots for Hg (II) acetate solutions (1 M in  $\text{Cl}^-$ ) at CNF/AuNPs electrodes. (B)  
292 Standard additions line for Hg (II) acetate additions to river water at CNFs/AuNPs electrodes. Values  
293 shown are the average of 3 measurements at independent electrodes.

294

### 295 3.3 Interference study

296 Solutions of 1  $\mu\text{M}$  Hg (II) acetate with 100  $\mu\text{M}$  of Pb (II), Cd (II), Zn (II) and  
297 Cu (II) were prepared to study the interference made by each one in comparison with a  
298 1  $\mu\text{M}$  mercury (II) acetate solution. CNF-AuNPs paper electrodes were used for Hg  
299 (II) quantification by the optimized procedure for the 1<sup>st</sup> UPD described in section 3.2.  
300 No variation of the oxidation peak intensity was observed, showing no signs of  
301 interference for these metals and confirming the selectivity of the method. All  
302 combinations were studied by triplicate.

303

304 The analytical characteristics reported in the literature for mercury ions  
305 determination by using paper devices are shown in Table 1. Most of mercury sensors in  
306 published paper-based devices are based on a colour change response due to the binding  
307 with specific ligands. These need normally higher quantity of reagents and more  
308 expensive detectors, limiting the portability. Electrochemical paper devices are more  
309 selective and the affinity with gold nanoparticles improves their sensitivity, but their

310 uses are still scarce. The sensor developed in this work has the advantages of using a  
311 fast and low-cost modification procedure. The electrodeposition of gold nanoparticles  
312 with the high conductivity of carbon nanomaterials allows reaching a limit of detection  
313 of 30 nM, suitable for safety control in waters. As an additional advantage, mercury  
314 stays in the cellulose fibers of the working paper electrode, and therefore the screen-  
315 printed platform can be reused without any contamination, reducing the analysis cost. In  
316 regard to waste management, the single-use paper electrode can be easily disposed,  
317 because of its small size.

## 318 INSERT TABLE 1

319 **Table 1:** Analytical characteristics of other paper devices described at the literature.

320

## 321 4. Conclusion

322 We tested the efficacy of an *easy-to-prepare* paper-based working electrode as a  
323 sensor for Hg (II) ions in river water, overlapping a screen-printed electrode as a  
324 connection system. The bare screen-printed electrode used remained free of mercury  
325 after the measurement. CNFs and rGO improve the conductivity of the electrode  
326 whereas electrodeposited AuNPs allow the sensitive and selective determination of Hg  
327 (II). By using the underpotential deposition of mercury on AuNPs, a limit of detection  
328 of 30 nM was obtained when both nanomaterials (CNFs and AuNPs) were used to  
329 modify the cellulose substrate. The determination was not affected by the presence of  
330 Zn (II), Cd (II), Pb (II) and Cu (II) ions. Mercury could be determined in spiked river  
331 samples (91% recovery and 6.2% RSD). The nanostructured paper-based electrode  
332 developed in this work could be the basis for a low-cost mercury sensor by  
333 electrochemical devices in paper platforms.

334

## 335 Acknowledgements

336 This work was supported by the Ministerio de Economía y Competitividad (MINECO,  
337 Spain), under the grant CTQ2013-47396-R, CTQ2011-25814, and the project  
338 CTQ2014-58826-R, MAT2017-84959-C2-1-R. This study was also financed by the  
339 Ministry of Economy and Employment of the Principality of Asturias (Plan of Science,  
340 Technology and Innovation 2013-2017), under the projects GRUPIN14-021 and  
341 GRUPIN14-022, IDI/2018/000185. Alberto Sánchez Calvo thanks the Ministry of  
342 Economy and Competitiveness for the award of a FPI Grant (BES-2015-072220).  
343 Support from the European Regional Development Fund (ERDF) is gratefully  
344 acknowledged.

345

346

347

348

349

350

351 **5. References**

- 352 [1] S. Lu, Y. Teng, Y. Wang, J. Wu, J. Wang, Research on the ecological risk of  
353 heavy metals in the soil around a Pb–Zn mine in the Huize County, China,  
354 Chinese J. Geochemistry. 34 (2015) 540–549. doi:10.1007/s11631-015-0062-6.
- 355 [2] E.A. Elkhatib, M.L. Moharem, Immobilization of copper, lead, and nickel in two  
356 arid soils amended with biosolids: effect of drinking water treatment residuals, J.  
357 Soils Sediments. 15 (2015) 1937–1946. doi:10.1007/s11368-015-1127-1.
- 358 [3] A. Kumar, R. Vij, M. Gupta, S. Sharma, S. Singh, Risk assessment of exposure  
359 to radon concentration and heavy metal analysis in drinking water samples in  
360 some areas of Jammu & Kashmir, India, J. Radioanal. Nucl. Chem. 304 (2015)  
361 1009–1016. doi:10.1007/s10967-015-3967-y.
- 362 [4] S.W. Teigen, R.A. Andersen, H.L. Daae, J.U. Skaare, Heavy metal content in  
363 liver and kidneys of grey seals (*Halichoerus grypus*) in various life stages  
364 correlated with metallothionein levels: Some metal-binding characteristics of this  
365 protein, Environ. Toxicol. Chem. 18 (1999) 2364–2369. doi:10.1897/1551-  
366 5028(1999)018<2364:HMCILA>2.3.CO;2.
- 367 [5] S. Malar, S. V. Sahi, P.J.C. Favas, P. Venkatachalam, Assessment of mercury  
368 heavy metal toxicity-induced physiochemical and molecular changes in *Sesbania*  
369 *grandiflora* L., Int. J. Environ. Sci. Technol. 12 (2014) 3273–3282.  
370 doi:10.1007/s13762-014-0699-4.
- 371 [6] M. Mutneja, Mercury toxicity and health effect, IJCS. 4 (2016) 96–100.
- 372 [7] A.L. Suherman, K. Ngamchuea, E.E.L. Tanner, S. V. Sokolov, J. Holter, N.P.  
373 Young, R.G. Compton, Electrochemical detection of ultratrace (Picomolar) levels  
374 of Hg<sup>2+</sup> using a silver nanoparticle-modified glassy carbon electrode, Anal.  
375 Chem. 89 (2017) 7166–7173. doi:10.1021/acs.analchem.7b01304.
- 376 [8] M.N. Rashed, Monitoring of contaminated toxic and heavy metals, from mine  
377 tailings through age accumulation, in soil and some wild plants at Southeast  
378 Egypt, J. Hazard. Mater. 178 (2010) 739–746.  
379 doi:10.1016/j.jhazmat.2010.01.147.
- 380 [9] X. Zhao, J. Wei, X. Shu, W. Kong, M. Yang, Multi-elements determination in  
381 medical and edible *Alpinia oxyphylla* and *Morinda officinalis* and their  
382 decoctions by ICP-MS, Chemosphere. 164 (2016) 430–435.  
383 doi:10.1016/j.chemosphere.2016.08.122.
- 384 [10] C. Locatelli, D. Melucci, Voltammetric determination of ultra-trace total mercury  
385 and toxic metals in meals, Food Chem. 130 (2012) 460–466.  
386 doi:10.1016/j.foodchem.2011.07.070.
- 387 [11] M. Powell, J.C. Ball, Y.-C. Tsai, M.F. Suárez, R.G. Compton, Square wave  
388 anodic stripping voltammetry at mercury-plated electrodes. Simulation of surface  
389 morphology effects on electrochemically reversible, irreversible, and quasi-

- 390 reversible processes: Comparison of thin films and microdroplets, *J. Phys. Chem.*  
391 *B.* 104 (2000) 8268–8278. doi:10.1021/jp001443s.
- 392 [12] L. Laffont, T. Hezard, P. Gros, L.E. Heimbürger, J.E. Sonke, P. Behra, D.  
393 Evrard, Mercury(II) trace detection by a gold nanoparticle-modified glassy  
394 carbon electrode using square-wave anodic stripping voltammetry including a  
395 chloride desorption step, *Talanta*. 141 (2015) 26–32.  
396 doi:10.1016/j.talanta.2015.03.036.
- 397 [13] T. Hezard, K. Fajerweg, D. Evrard, V. Collière, P. Behra, P. Gros, Influence of  
398 the gold nanoparticles electrodeposition method on Hg(II) trace electrochemical  
399 detection, *Electrochim. Acta*. 73 (2012) 15–22.  
400 doi:10.1016/j.electacta.2011.10.101.
- 401 [14] M. Colilla, M.A. Mendiola, J.R. Procopio, M.T. Sevilla, Application of a carbon  
402 paste electrode modified with a Schiff base ligand to mercury speciation in water,  
403 *Electroanalysis*. 17 (2005) 933–940. doi:10.1002/elan.200403198.
- 404 [15] J. Wu, L. Li, B. Shen, G. Cheng, P. He, Y. Fang, Polythymine oligonucleotide-  
405 modified gold electrode for voltammetric determination of mercury(II) in  
406 aqueous solution, *Electroanalysis*. 22 (2010) 479–482.  
407 doi:10.1002/elan.200900441.
- 408 [16] D. Wu, Q. Zhang, X. Chu, H. Wang, G. Shen, R. Yu, Ultrasensitive  
409 electrochemical sensor for mercury (II) based on target-induced structure-  
410 switching DNA, *Biosens. Bioelectron.* 25 (2010) 1025–1031.  
411 doi:10.1016/j.bios.2009.09.017.
- 412 [17] M. Vasjari, Y.M. Shirshov, A. V. Samoylov, V.M. Mirsky, SPR investigation of  
413 mercury reduction and oxidation on thin gold electrodes, *J. Electroanal. Chem.*  
414 605 (2007) 73–76. doi:10.1016/j.jelechem.2007.03.019.
- 415 [18] M. Shamsipur, A. Safavi, Z. Mohammadpour, R. Ahmadi, Highly selective  
416 aggregation assay for visual detection of mercury ion based on competitive  
417 binding of sulfur-doped carbon nanodots to gold nanoparticles and mercury ions,  
418 *Microchim. Acta*. 183 (2016) 2327–2335. doi:10.1007/s00604-016-1870-z.
- 419 [19] K. Kiran, Gold nanoparticles for mercury determination in environmental water  
420 and vegetable samples, *Appl. Nanosci.* 5 (2015) 361–366. doi:10.1007/s13204-  
421 014-0325-2.
- 422 [20] E. B. Santos, S. Ferlin, A. H. Fostier, I. O. Mazali, Using gold nanoparticles as  
423 passive sampler for indoor monitoring of Gaseous Elemental Mercury, *J. Braz.*  
424 *Chem. Soc.* 28 (2017) 1274–1280.
- 425 [21] N. Zohora, D. Kumar, M. Yazdani, V.M. Rotello, R. Ramanathan, V. Bansal,  
426 Rapid colorimetric detection of mercury using biosynthesized gold nanoparticles,  
427 *Colloids Surfaces A Physicochem. Eng. Asp.* (2017) 1–7.  
428 doi:10.1016/j.colsurfa.2017.04.036.
- 429 [22] V.V. Kumar, S.P. Anthony, Highly selective colorimetric sensing of Hg<sup>2+</sup> ions  
430 by label free AuNPs in aqueous medium across wide pH range, *Sensors*  
431 *Actuators, B Chem.* 225 (2016) 413–419. doi:10.1016/j.snb.2015.11.079.
- 432 [23] T. Hezard, K. Fajerweg, D. Evrard, V. Collire, P. Behra, P. Gros, Gold

- 433 nanoparticles electrodeposited on glassy carbon using cyclic voltammetry:  
434 Application to Hg(II) trace analysis, *J. Electroanal. Chem.* 664 (2012) 46–52.  
435 doi:10.1016/j.jelechem.2011.10.014.
- 436 [24] N. Wang, M. Lin, H. Dai, H. Ma, Functionalized gold nanoparticles/reduced  
437 graphene oxide nanocomposites for ultrasensitive electrochemical sensing of  
438 mercury ions based on thymine-mercury-thymine structure, *Biosens. Bioelectron.*  
439 79 (2016) 320–326. doi:10.1016/j.bios.2015.12.056.
- 440 [25] E.C. Rama, M.B. González-García, A. Costa-García, Competitive  
441 electrochemical immunosensor for amyloid-beta 1-42 detection based on gold  
442 nanostructured Screen-Printed Carbon Electrodes, *Sensors Actuators, B Chem.*  
443 201 (2014) 567–571. doi:10.1016/j.snb.2014.05.044.
- 444 [26] M.A. Kamyabi, A. Aghaei, Electromembrane extraction and anodic stripping  
445 voltammetric determination of mercury(II) using a glassy carbon electrode  
446 modified with gold nanoparticles, *Microchim. Acta.* 183 (2016) 2411–2419.  
447 doi:10.1007/s00604-016-1884-6.
- 448 [27] İ. Üstündağ, A. Erkal, T. Koralay, Y.K. Kadioğlu, S. Jeon, Gold nanoparticle  
449 included graphene oxide modified electrode: Picomole detection of metal ions in  
450 seawater by stripping voltammetry, *ISSN J. Anal. Chem.* 71 (2016) 1061–9348.  
451 doi:10.1134/S1061934816070108.
- 452 [28] E. Fernández, L. Vidal, D. Martín-Yerga, M.D.C. Blanco, A. Canals, A. Costa-  
453 García, Screen-printed electrode based electrochemical detector coupled with  
454 ionic liquid dispersive liquid-liquid microextraction and microvolume back-  
455 extraction for determination of mercury in water samples, *Talanta.* 135 (2015)  
456 34–40. doi:10.1016/j.talanta.2014.11.069.
- 457 [29] D. Martín-Yerga, I. Álvarez-Martos, M.C. Blanco-López, C.S. Henry, M.T.  
458 Fernández-Abedul, Point-of-need simultaneous electrochemical detection of lead  
459 and cadmium using low-cost stencil-printed transparency electrodes, *Anal. Chim.*  
460 *Acta.* 981 (2017) 24–33. doi:10.1016/j.aca.2017.05.027.
- 461 [30] M.P.N. Bui, J. Brockgreitens, S. Ahmed, A. Abbas, Dual detection of nitrate and  
462 mercury in water using disposable electrochemical sensors, *Biosens. Bioelectron.*  
463 85 (2016) 280–286. doi:10.1016/j.bios.2016.05.017.
- 464 [31] E. Núñez-Bajo, M. Carmen Blanco-López, A. Costa-García, M. Teresa  
465 Fernández-Abedul, Integration of gold-sputtered electrofluidic paper on wire-  
466 included analytical platforms for glucose biosensing, *Biosens. Bioelectron.* 91  
467 (2017) 824–832. doi:10.1016/j.bios.2017.01.029.
- 468 [32] W. Dungchai, O. Chailapakul, C.S. Henry, Electrochemical detection for paper-  
469 based microfluidics, *Anal. Chem.* 81 (2009) 5821–5826. doi:10.1021/ac9007573.
- 470 [33] A.W. Martinez, S.T. Phillips, M.J. Butte, G.M. Whitesides, Patterned paper as a  
471 platform for inexpensive, low-volume, portable bioassays, *Angew. Chemie - Int.*  
472 *Ed.* 46 (2007) 1318–1320. doi:10.1002/anie.200603817.
- 473 [34] E. Nunez-Bajo, M.C. Blanco-López, A. Costa-García, M.T. Fernández-Abedul,  
474 Electrogeneration of gold nanoparticles on porous-carbon paper-based electrodes  
475 and application to inorganic arsenic analysis in white wines by  
476 chronoamperometric stripping, *Anal. Chem.* 89 (2017) 6415–6423.

477 doi:10.1021/acs.analchem.7b00144.

478 [35] O. Amor-Gutiérrez, E. Costa Rama, A. Costa-García, M.T. Fernández-Abedul,  
479 Paper-based maskless enzymatic sensor for glucose determination combining ink  
480 and wire electrodes, *Biosens. Bioelectron.* 93 (2017) 40–45.  
481 doi:10.1016/j.bios.2016.11.008.

482 [36] E. Núñez-Bajo, M.C. Blanco-López, A. Costa-García, M.T. Fernández-Abedul,  
483 In situ gold-nanoparticle electrogeneration on gold films deposited on paper for  
484 non-enzymatic electrochemical determination of glucose, *Talanta.* 178 (2018)  
485 160–165. doi:10.1016/j.talanta.2017.08.104.

486 [37] A.S. Calvo, C. Botas, D. Martín-Yerga, P. Álvarez, R. Menéndez, A. Costa-  
487 García, Comparative study of screen-printed electrodes modified with graphene  
488 oxides reduced by a constant current, *J. Electrochem. Soc.* 162 (2015) B282–  
489 B290. doi:10.1149/2.1021510jes.

490 [38] A. Sánchez-Calvo, E. Núñez-Bajo, M.T. Fernández-Abedul, M.C. Blanco-López,  
491 A. Costa García, Optimization and characterization of nanostructured paper-  
492 based electrodes, *Electrochim. Acta.* 265 (2018) 717–725.  
493 doi:10.1016/j.electacta.2018.01.179.

494 [39] D. Martín-Yerga, M.B. González-García, A. Costa-García, Use of nanohybrid  
495 materials as electrochemical transducers for mercury sensors, *Sensors Actuators,*  
496 *B Chem.* 165 (2012) 143–150. doi:10.1016/j.snb.2012.02.031.

497 [40] E. Herrero, H.D. Abruna, Underpotential deposition of mercury on Au(111):  
498 Electrochemical studies and comparison with structural investigations, *Langmuir.*  
499 13 (1997) 4446–4453. doi:10.1021/la970109t.

500 [41] K. Jüttner, Electrochemical impedance spectroscopy (EIS) of corrosion processes  
501 on inhomogeneous surfaces, *Electrochim. Acta.* 35 (1990) 1501–1508.  
502 doi:10.1016/0013-4686(90)80004-8.

503 [42] L. Feng, X. Li, H. Li, W. Yang, L. Chen, Y. Guan, Enhancement of sensitivity of  
504 paper-based sensor array for the identification of heavy-metal ions, *Anal. Chim.*  
505 *Acta.* 780 (2013) 74–80. doi:10.1016/j.aca.2013.03.046.

506 [43] G.H. Chen, W.Y. Chen, Y.C. Yen, C.W. Wang, H.T. Chang, C.F. Chen,  
507 Detection of mercury(II) ions using colorimetric gold nanoparticles on paper-  
508 based analytical devices, *Anal. Chem.* 86 (2014) 6843–6849.  
509 doi:10.1021/ac5008688.

510 [44] Y.-X. Qi, M. Zhang, A. Zhu, G. Shi, Terbium( iii )/gold nanocluster conjugates:  
511 the development of a novel ratiometric fluorescent probe for mercury( ii ) and a  
512 paper-based visual sensor, *Analyst.* 140 (2015) 5656–5661.  
513 doi:10.1039/C5AN00802F.

514

515



**Fig. 1** Schematic diagram showing the preparation of the paper electrodes used. (A) Modification of cellulose substrate by addition of carbon ink on one side, having the platform two visually different sides. Solution is added with a micropipette through the upper side. (B) Overlapping process of the bottom (ink) side of the paper electrode on the screen-printed card. (C) Modification of the paper electrode with 1) CNFs and AuNPs, and 2) rGO and AuNPs.

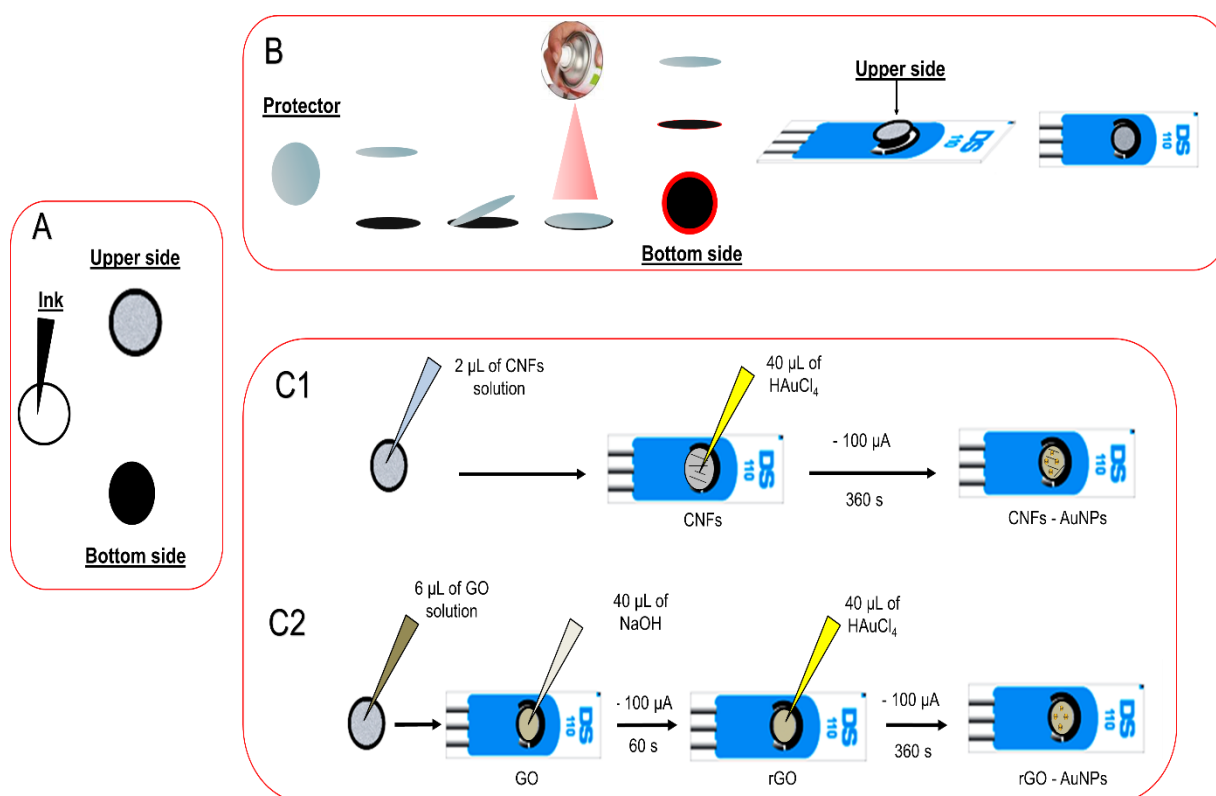


**Fig. 2** Cyclic voltammograms obtained at CNFs/AuNPs electrodes in a  $10^{-4}$  M Hg (II) acetate solution in (A) 0.1 M HCl, (B) 0.1 M HCl + 0.9 M KCl and (C) 0.1 M HCl + 1.9 M KCl solutions. (D) Background voltammogram recorded in a 0.1 M HCl + 0.9 M KCl solution.

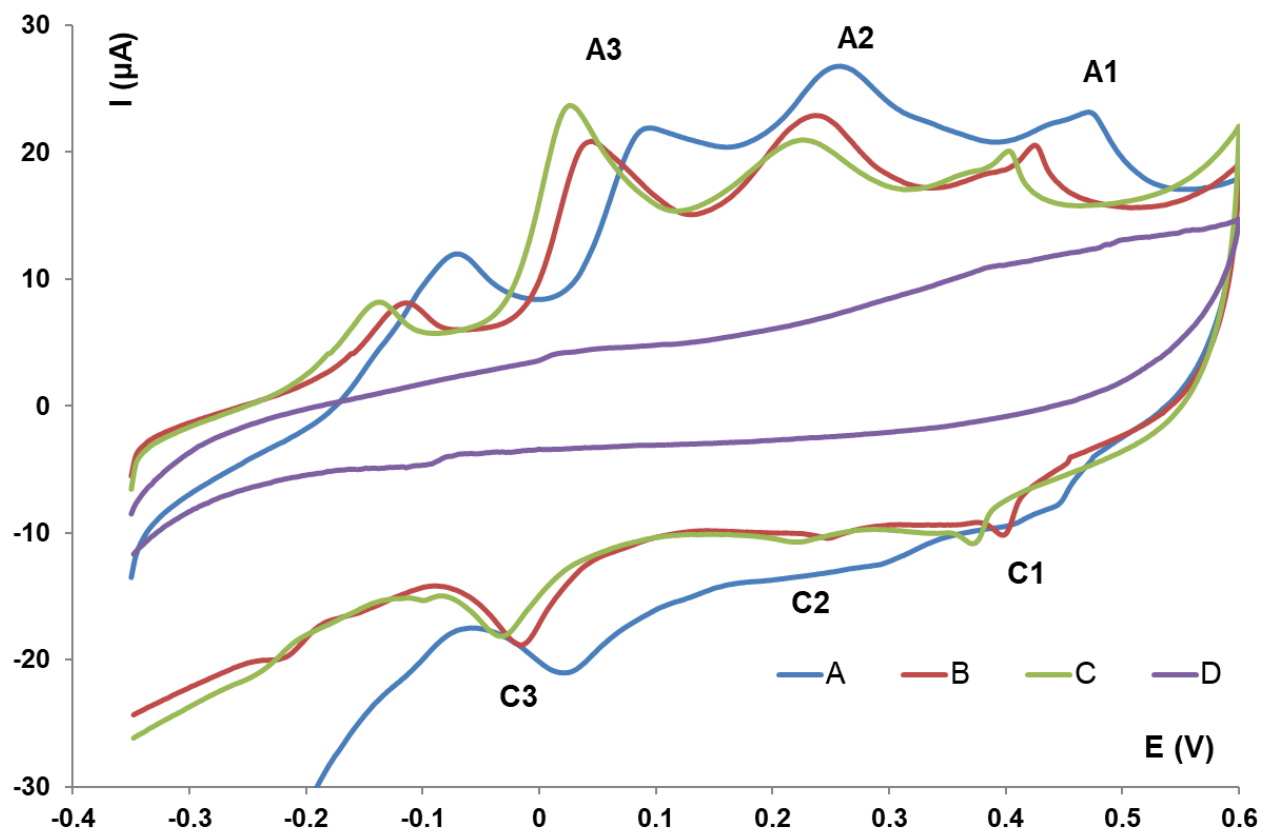


**Fig. 3** Cyclic voltammograms for a  $10^{-4}$  M Hg (II) acetate solution at A) CNFs/AuNPs, (B) CNFs, (C) rGO/AuNPs and (D) rGO modified electrodes. Background electrolyte: 0.1 M HCl + 0.9 M KCl solution.

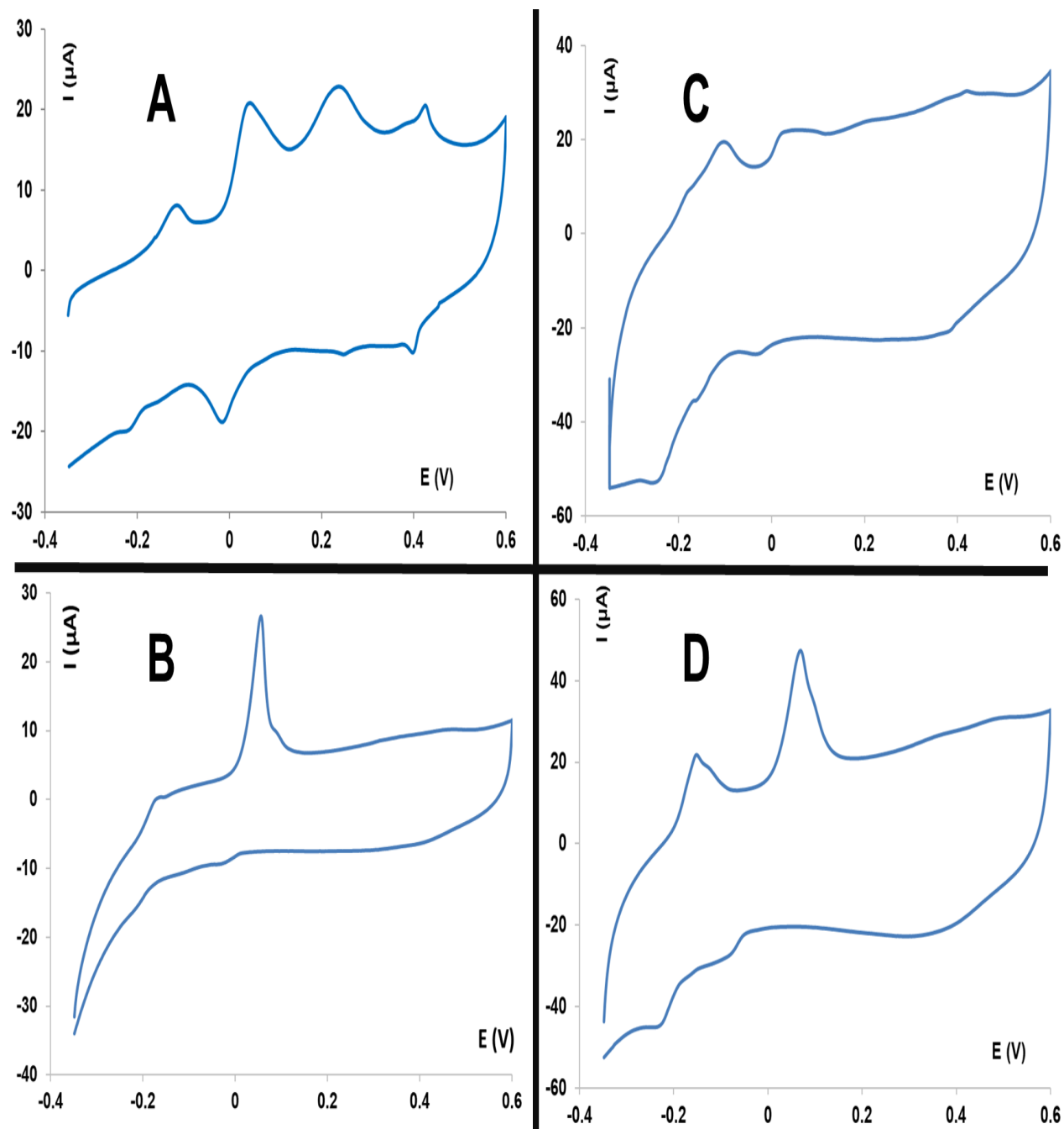


**Fig. 4** (A) Calibration plots for **Hg (II)** acetate in CNF/AuNPs and rGO/AuNPs paper-based electrodes. (B) Linear sweep voltammograms in CNF/AuNPs paper-based electrodes at different concentrations of mercury (II) acetate in a 0.1 M HCl + 0.9 M KCl solution.

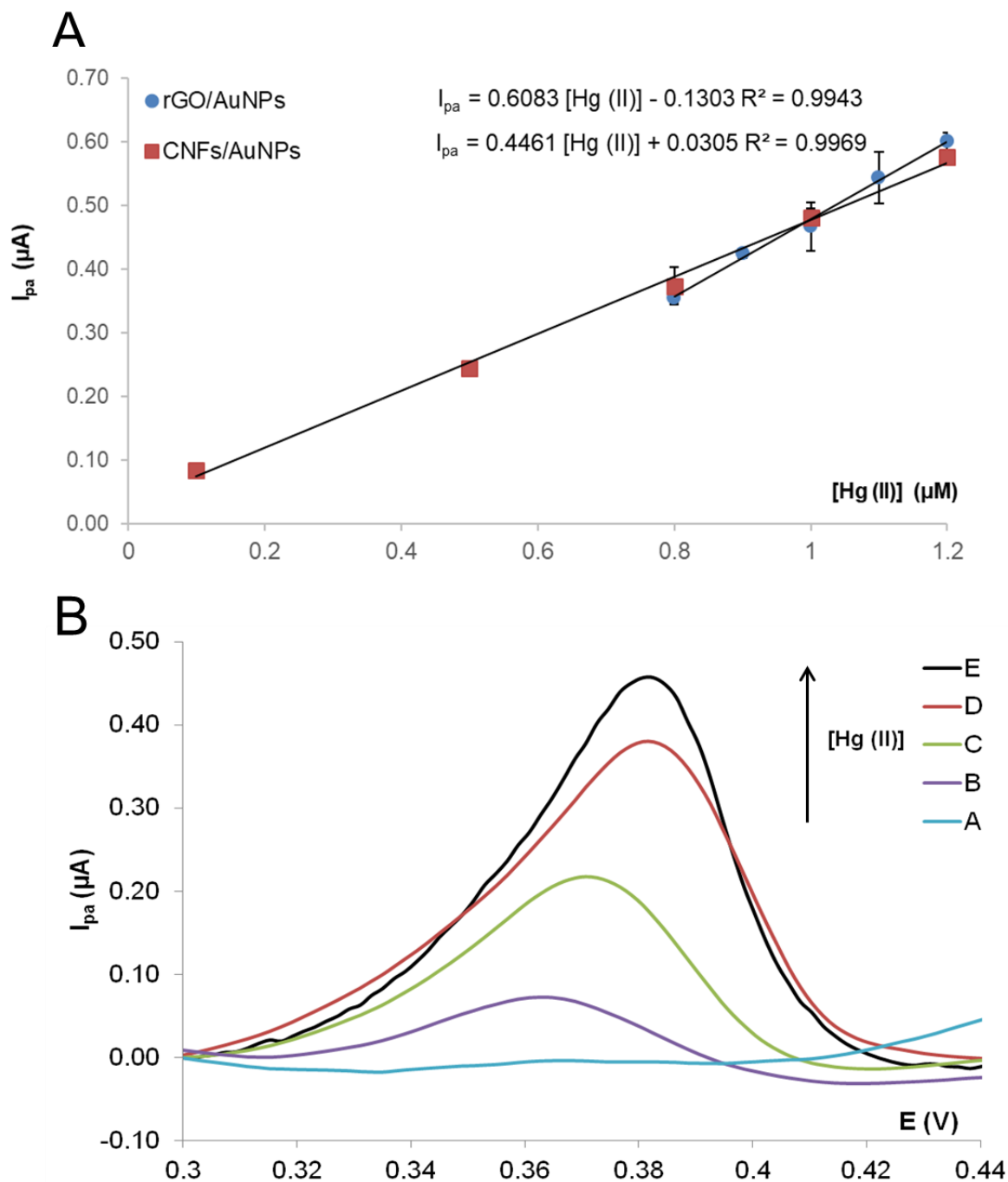


**Fig. 5** (A) Calibration plots for Hg (II) acetate solutions (1 M in Cl<sup>-</sup>) at CNF/AuNPs electrodes. (B) Standard additions line for Hg (II) acetate additions to river water at CNFs/AuNPs electrodes. Values shown are the average of 3 measurements at independent electrodes.

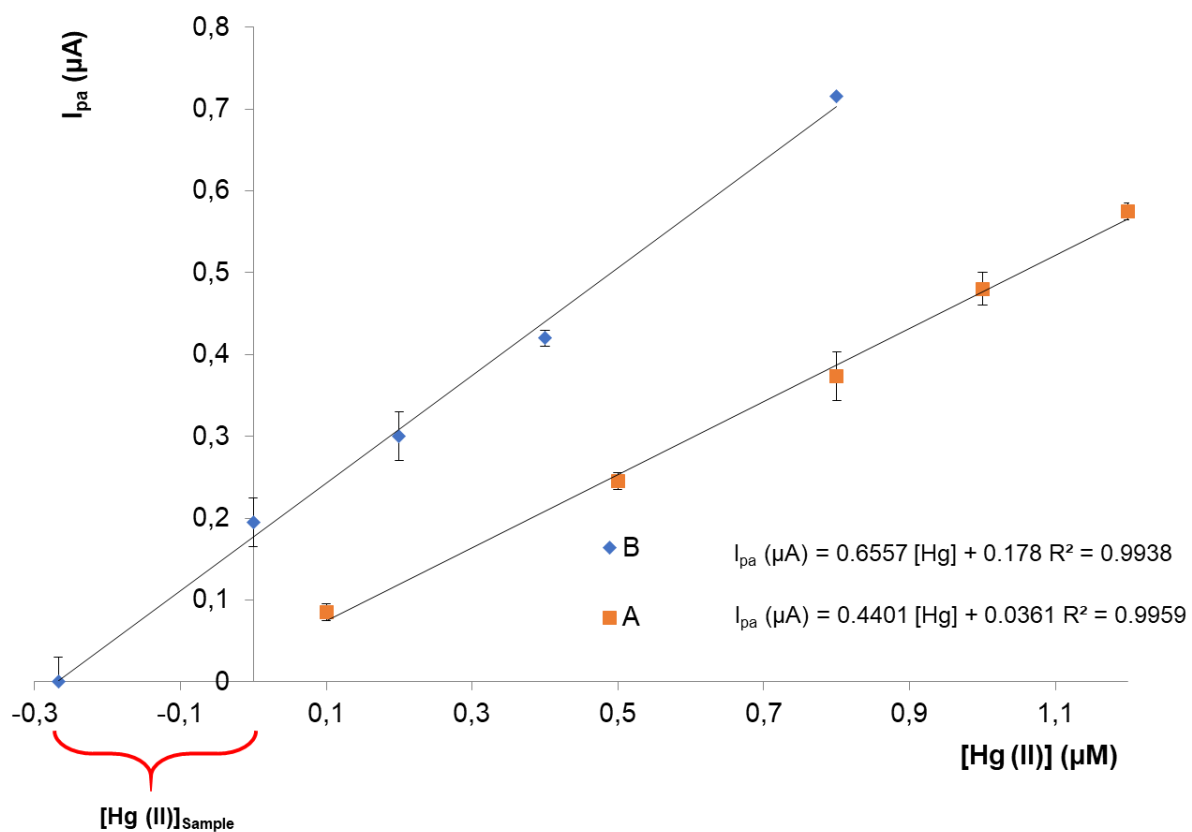


**Table 1.** Analytical characteristics of other paper devices described at the literature for Hg (II) determination.

Sensor	Analytical signal	Range ( $\mu\text{M}$ )	LOD ( $\mu\text{M}$ )
Array for multi-heavy metal ions [42]	Colour change	10-50	10
Gold nanoparticles paper-based device [43]	Colour change	0.025-0.75	0.05
Terbium/gold nanocluster [44]	Fluorescence	0.005-7	0.01
Dual detection of nitrate and mercury with AuNPs [30]	Electrochemical (DPV)	0.07-17.5	0.005
CNFs /AuNPs (this work)	Electrochemical (LSV)	0.1-1.2	0.03